ELSEVIER

Computer Physics Communications 147 (2002) 7–12

Computer Physics Communications

www.elsevier.com/locate/cpc

Modeling nematohydrodynamics in liquid crystal devices

Géza Tóth [a], Colin Denniston [b], J.M. Yeomans [a,*]

[a] *Department of Physics, University of Oxford, Theoretical Physics, 1 Keble Road, Oxford OX1 3NP, UK*
[b] *Department of Physics and Astronomy, The Johns Hopkins University, Baltimore, MD 21218, USA*

Abstract

We formulate a lattice Boltzmann algorithm which solves the hydrodynamic equations of motion for nematic liquid crystals. The applicability of the approach is demonstrated by presenting results for two liquid crystal devices where flow has an important role to play in the switching.

PACS: 47.11.+j; 61.30.Gd; 83.80.Xz; 85.60.Pg

Keywords: Lattice Boltzmann; Liquid crystals; Display devices

1. Introduction

In this paper we describe a lattice Boltzmann algorithm which solves the hydrodynamic equations of motion for nematic liquid crystals. Liquid crystals are widely used in display devices and, as examples of applications of the algorithm, we consider two model devices where flow has an important role to play in the switching.

Liquid crystals are fluids made up of rod-shaped molecules [1]. At high temperatures and low concentrations the angular distribution of the molecules is isotropic. However, as the temperature is lowered or the concentration increased, a liquid crystal can undergo a phase transition to a state where the molecules tend to align in parallel, the so-called nematic phase. Liquid crystals exhibit complicated, non-Newtonian flow behaviour because of the coupling between this molecular structure and the flow field [2]. Examples include shear thinning and non-equilibrium phase transitions such as banding under shear [3].

Another consequence of the ordering of nematic liquid crystals is their widespread use in optical display devices such as those on digital watches or calculators. In a typical display device, the liquid crystal is confined between two plates a few microns apart. The molecular configuration on the plates is fixed. When an electric field is switched on molecules in the bulk align in the direction preferred by the field. After switching off the field, long-range elastic interactions ensure that the molecules reorient themselves in the direction preferred by the surfaces. These devices can be used as displays because different liquid crystal orientations have different optical properties. Flow can be important in device operation because it can control the speed of switching or even select the states between which switching can occur.

Modeling flow in non-Newtonian fluids such as liquid crystals is difficult because of the need to incorporate the coupling between the microscopic structure and the flow. The hydrodynamic equations of mo-

* Corresponding author.
E-mail address: yeomans@thphys.ox.ac.uk (J.M. Yeomans).

0010-4655/02/$ – see front matter
PII: S0010-4655(02)00196-0

tion can be extremely complex and numerical solutions demanding. A method which has recently proved very successful in modeling complex fluids is the lattice Boltzmann approach [4]. Lattice Boltzmann simulations solve the hydrodynamic equations of motion while retaining sufficient, albeit generic, molecular information to model the important physics of a given fluid. This is often done by imposing a Landau free energy functional, so the fluid evolves to a known thermodynamic equilibrium [5]. The method has been successfully used to investigate domain growth in binary mixtures and liquid–gas systems [6], the flow of binary mixtures in porous media, and ordering in amphiphilic fluids [7].

Here we construct a lattice Boltzmann algorithm to solve the hydrodynamic equations of motion for nematic liquid crystals. We follow Beris and Edwards [8] and consider a rather general formalism of the hydrodynamics written in terms of a tensor order parameter, **Q**. This approach lends itself to a lattice Boltzmann interpretation: the partial density distribution functions which are the usual variables in the simulations are supplemented by a set of tensors related to **Q**. Backflow, the hydrodynamics of topological defects and the possibility of transitions between the nematic and isotropic phases appear naturally within the formalism.

The next section of the paper summarizes the Beris–Edwards equations of motion for liquid crystal hydrodynamics. Section 3 describes the lattice Boltzmann algorithm. General viscosity terms, needed to match to experimental viscosities, are included. The approach is applied to switching in a Frederiks cell in Section 4 and, in Section 5, used to confirm that backflow can influence state selection in a bistable liquid crystal device.

2. Hydrodynamic equations of motion

Ordering in a nematic liquid crystal can be described in terms of a tensor order parameter **Q** which is symmetric and traceless. Expanding the free energy in terms of the order parameter gives the Landau–de-Gennes expression [1]

$$\mathfrak{F} = \int_V \mathrm{d}V\,\{F_b - F_E + F_d\} + \int_{\partial V} \mathrm{d}S\,\{F_a\}, \tag{1}$$

where

$$\begin{aligned} F_b &= \frac{A}{2}\left(1-\frac{\gamma}{3}\right)Q_{\alpha\beta}^2 - \frac{A\gamma}{3}Q_{\alpha\beta}Q_{\beta\gamma}Q_{\gamma\alpha} \\ &\quad + \frac{A\gamma}{4}\left(Q_{\alpha\beta}^2\right)^2, \\ F_d &= \frac{L_1}{2}(\partial_\alpha Q_{\beta\gamma})^2 + \frac{L_2}{2}(\partial_\alpha Q_{\alpha\gamma})(\partial_\beta Q_{\beta\gamma}) \\ &\quad + \frac{L_3}{2}Q_{\alpha\beta}(\partial_\alpha Q_{\gamma\epsilon})(\partial_\beta Q_{\gamma\epsilon}), \\ F_a &= \frac{\alpha_s}{2}\left(Q_{\alpha\beta}-Q_{\alpha\beta}^0\right)^2, \qquad F_E = \frac{\epsilon_a}{12\pi}E_\alpha Q_{\alpha\beta}E_\beta. \end{aligned} \tag{2}$$

(Greek subscripts represent Cartesian directions and the usual summation over repeated indices is assumed.) The bulk free energy terms F_b describe a liquid crystal with a first-order, isotropic–nematic transition at $\gamma = 2.7$ [9]. Contributions to the free energy which arise from an imposed electric field $\boldsymbol{E}$ are included in F_E. F_d describes the elastic free energy [8] and F_a is a surface free energy which fixes a preferred orientation $\mathbf{Q}^0$ for the surface director field.

Q evolves according to a convection-diffusion equation [8]

$$(\partial_t + \boldsymbol{u}\cdot\nabla)\mathbf{Q} - \mathbf{S}(\mathbf{W},\mathbf{Q}) = \Gamma\mathbf{H}, \tag{3}$$

where $\boldsymbol{u}$ is the bulk fluid velocity and Γ is a collective rotational diffusion constant. The term on the right-hand side of Eq. (3) describes the relaxation of the order parameter towards the minimum of the free energy $\mathfrak{F}$,

$$\mathbf{H} = -\frac{\delta\mathfrak{F}}{\delta\mathbf{Q}} + (\mathbf{I}/3)\,\mathrm{Tr}\left\{\frac{\delta\mathfrak{F}}{\delta\mathbf{Q}}\right\}. \tag{4}$$

The order parameter distribution can be both rotated and stretched by flow gradients. This is described by the term on the left-hand side

$$\begin{aligned} \mathbf{S}(\mathbf{W},\mathbf{Q}) &= (\xi\mathbf{D}+\Omega)(\mathbf{Q}+\mathbf{I}/3) \\ &\quad + (\mathbf{Q}+\mathbf{I}/3)(\xi\mathbf{D}-\Omega) \\ &\quad - 2\xi(\mathbf{Q}+\mathbf{I}/3)\,\mathrm{Tr}(\mathbf{QW}), \end{aligned} \tag{5}$$

where $\mathbf{D} = (\mathbf{W}+\mathbf{W}^{\mathrm{T}})/2$ and $\Omega = (\mathbf{W}-\mathbf{W}^{\mathrm{T}})/2$ are the symmetric part and the anti-symmetric part, respectively, of the velocity gradient tensor $W_{\alpha\beta} = \partial_\beta u_\alpha$ and ξ is related to the aspect ratio of the molecules.

The flow of the liquid crystal fluid obeys the continuity and Navier–Stokes equations

$$\partial_t\rho + \partial_\alpha\rho u_\alpha = 0, \tag{6}$$

$$\rho\partial_t u_\alpha + \rho u_\beta \partial_\beta u_\alpha = \partial_\beta \sigma_{\alpha\beta} + \frac{\rho\tau_f}{3}\partial_\beta\big((\delta_{\alpha\beta} + 3\partial_n \sigma_{\alpha\beta})\partial_\zeta u_\zeta + \partial_\alpha u_\beta + \partial_\beta u_\alpha\big), \tag{7}$$

where

$$\begin{aligned}\sigma_{\alpha\beta} = {} & -\rho T\delta_{\alpha\beta} - (\xi-1)H_{\alpha\gamma}\big(Q_{\gamma\beta} + \tfrac{1}{3}\delta_{\gamma\beta}\big) \\ & - (\xi+1)\big(Q_{\alpha\gamma} + \tfrac{1}{3}\delta_{\alpha\gamma}\big)H_{\gamma\beta} \\ & + 2\xi\big(Q_{\alpha\beta} + \tfrac{1}{3}\delta_{\alpha\beta}\big)Q_{\gamma\epsilon}H_{\gamma\epsilon} \\ & - \partial_\beta Q_{\gamma\nu}\frac{\delta\mathfrak{F}}{\delta\partial_\alpha Q_{\gamma\nu}} \\ & + \beta\big(Q_{\alpha\beta} + \tfrac{1}{3}\delta_{\alpha\beta}\big)Q_{\gamma\epsilon}W_{\gamma\epsilon} + \sigma_{M,\alpha\beta}\end{aligned} \tag{8}$$

is the stress due to the nematic order [8] and the external electric field. The latter is represented by the $\sigma_{M,\alpha\beta}$ Maxwell stress tensor [10].

3. Lattice Boltzmann algorithm

A lattice Boltzmann scheme which reproduces Eqs. (3), (6) and (7) to second order can be defined in terms of two distribution functions $f_i(\boldsymbol{x})$ and $\mathbf{G}_i(\boldsymbol{x})$ where i labels lattice directions from site $\boldsymbol{x}$. Physical variables are related to the distribution functions by

$$\rho = \sum_i f_i, \quad \rho u_\alpha = \sum_i f_i e_{i\alpha}, \quad \mathbf{Q} = \sum_i \mathbf{G}_i. \tag{9}$$

The distribution functions evolve in a time step Δt according to

$$\begin{aligned}&\big(f_i(\boldsymbol{x}+\boldsymbol{e}_i\Delta t, t+\Delta t) - f_i(\boldsymbol{x},t)\big)/\Delta t \\ &\quad = \tfrac{1}{2}\big[\mathcal{C}_{fi}\big(\boldsymbol{x},t,\{f_i\}\big) + \mathcal{C}_{fi}\big(\boldsymbol{x}+\boldsymbol{e}_i\Delta t, t+\Delta t, \{f_i^*\}\big)\big], \\ &\big(\mathbf{G}_i(\boldsymbol{x}+\boldsymbol{e}_i\Delta t, t+\Delta t) - \mathbf{G}_i(\boldsymbol{x},t)\big)/\Delta t \\ &\quad = \frac{\mathcal{C}_{\mathbf{G}i}(\boldsymbol{x},t,\{\mathbf{G}_i\}) + \mathcal{C}_{\mathbf{G}i}(\boldsymbol{x}+\boldsymbol{e}_i\Delta t, t+\Delta t, \{\mathbf{G}_i^*\})}{2},\end{aligned} \tag{10}$$

where the collision operators are taken to have the form of a single relaxation time Boltzmann equation, together with a forcing term

$$\begin{aligned}&\mathcal{C}_{fi}\big(\boldsymbol{x},t,\{f_i\}\big) \\ &\quad = -\frac{f_i(\boldsymbol{x},t) - f_i^0(\boldsymbol{x},t,\{f_i\})}{\tau_f} + p_i\big(\boldsymbol{x},t,\{f_i\}\big), \\ &\mathcal{C}_{\mathbf{G}i}\big(\boldsymbol{x},t,\{\mathbf{G}_i\}\big) \\ &\quad = -\frac{\mathbf{G}_i(\boldsymbol{x},t) - \mathbf{G}_i^0(\boldsymbol{x},t,\{\mathbf{G}_i\})}{\tau_{\mathbf{G}}} + h_i\big(\boldsymbol{x},t,\{\mathbf{G}_i\}\big).\end{aligned} \tag{11}$$

f_i^* and $\mathbf{G}_i^*$ in Eqs. (10) and (11) are first order approximations to $f_i(\boldsymbol{x}+\boldsymbol{e}_i\Delta t, t+\Delta t)$ and $\mathbf{G}_i(\boldsymbol{x}+\boldsymbol{e}_i\Delta t, t+\Delta t)$. They are introduced to remove lattice viscosity terms to second order and they give improved stability.

The form of the equations of motion and thermodynamic equilibrium follows from the choice of the moments of the equilibrium distributions f_i^0 and $\mathbf{G}_i^0$ and the driving terms p_i and h_i. f_i^0 is constrained by

$$\begin{aligned}&\sum_i f_i^0 = \rho, \qquad \sum_i f_i^0 e_{i\alpha} = \rho u_\alpha, \\ &\sum_i f_i^0 e_{i\alpha} e_{i\beta} = -\sigma_{\alpha\beta}^s + \rho u_\alpha u_\beta,\end{aligned} \tag{12}$$

where the zeroth and first moments are chosen to impose conservation of mass and momentum. The second moment of f^0 controls the symmetric part of the stress tensor, whereas the moments of p_i

$$\begin{aligned}&\sum_i p_i = 0, \qquad \sum_i p_i e_{i\alpha} = \partial_\beta \sigma_{\alpha\beta}^a, \\ &\sum_i p_i e_{i\alpha} e_{i\beta} = 0\end{aligned} \tag{13}$$

impose the antisymmetric part of the stress tensor.

For the equilibrium of the order parameter distribution we choose

$$\begin{aligned}&\sum_i \mathbf{G}_i^0 = \mathbf{Q}, \qquad \sum_i \mathbf{G}_i^0 e_{i\alpha} = \mathbf{Q}u_\alpha, \\ &\sum_i \mathbf{G}_i^0 e_{i\alpha} e_{i\beta} = \mathbf{Q}u_\alpha u_\beta.\end{aligned} \tag{14}$$

This ensures that the fluid minimizes its free energy at equilibrium and that it is convected with the flow. Finally the evolution of the order parameter is most conveniently modeled by choosing

$$\sum_i h_i = \Gamma \mathbf{H}(\mathbf{Q}) + \mathbf{S}(\mathbf{W}, \mathbf{Q}),$$
$$\sum_i h_i e_{i\alpha} = \left(\sum_i h_i \right) u_\alpha. \tag{15}$$

Conditions (12)–(15) can be satisfied by taking f_i^0, $\mathbf{G}_i^0$, h_i, and p_i as polynomial expansions in the velocity as is usual in lattice Boltzmann schemes [4]. A second-order Chapman–Enskog expansion for the evolution equations (10) incorporating the conditions (12)–(15) leads to the equations of motion [11].

4. Frederiks cell

One of the simplest liquid crystal devices is the Frederiks cell depicted in Fig. 1. When the voltage is increased above a critical value V_c switching from the zero voltage state occurs rather rapidly. The factor limiting the speed at which the device can be updated is the switching from the voltage-aligned state to that preferred by the boundaries. This switching involves both relaxation of the free energy and viscous dissipation associated with hydrodynamic modes [1]. Our aim is to quantitatively model this phenomenon for a given set of elastic constants and viscosities [12].

Fig. 2 shows θ, the director angle [13] measured in the centre of the channel, as indicated in Fig. 1, as a function of time as the voltage is switched on and then

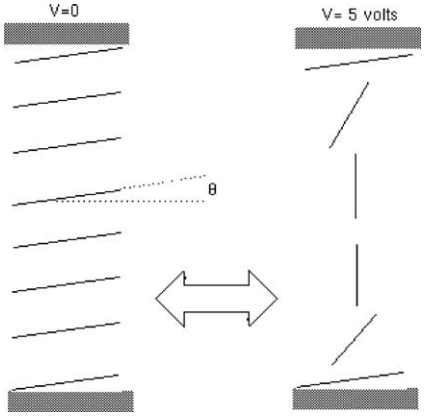

Fig. 1. The two stable states of a Frederiks cell. At zero voltage the liquid crystal prefers the orientation imposed by the boundaries. When the electric field is turned on the nematic prefers to align along the field direction.

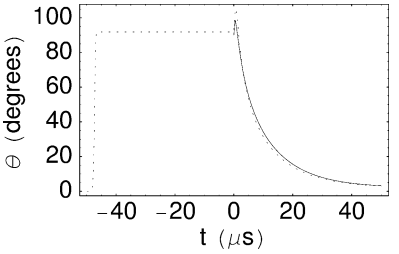

Fig. 2. Angle θ, with the horizontal, of the director at the centre of the cell as a function of time. The system starts in the fully relaxed, zero voltage state and the voltage is turned on immediately at the far left of the plot. The voltage is turned off at $t = 0$.

off. The parameters used for the simulation are listed in footnote [14] and were chosen to correspond to commercially relevant materials. For comparison, we show relaxation data, provided by Sharp Laboratories of Europe, taken from a simulation using a commercial code which solves the Ericksen–Leslie [15] equations in one dimension. (For a similar, but not identical, Ericksen–Leslie calculation and comparison to experimental data see Ref. [16].) For the most part, there is very good agreement between the two methods.

The "blip" seen in the plot when the voltage is turned off is a real effect known as the optical bounce, due to its optical signature. After the removal of the electric field, the changing director field induces a hydrodynamic flow. This, in turn, couples back to the director field and causes it to momentarily move in the "wrong" direction. Viscous dissipation in the fluid rapidly damps out the flow and the director can then relax toward the minimum of the free energy. The bounce we see is somewhat higher than that observed in the Ericksen–Leslie simulations. However recent attempts to exactly match the quantitative features of the optical bounce to solutions of the Ericksen–Leslie equations have suggested that they always underestimate its value relative to experiments [16]. Thus, the additional details in the tensor model may be better in reproducing the experimental results.

5. Flow-induced surface switching

A current aim of the device industry is to construct bistable displays which can remain in two different (meta)stable states for zero field. This would, for example, lead to significant power saving in infrequently

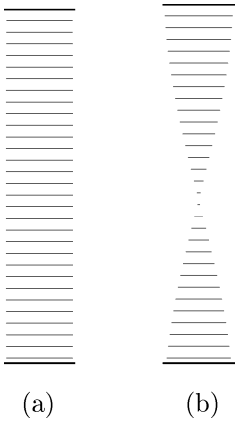

Fig. 3. The two stable states (a) horizontal and (b) twist of the surface switching device considered in Section 5. In (b) the molecular orientation twists to perpendicular to the plane of the figure at the middle of the sample.

updated displays or could be used in the construction of smart cards which rely on an external power source.

In this paper we will consider one possible mechanism for accessing two zero-field states, flow-induced surface switching [17]. The two states are the horizontal and the twist states shown in Fig. 3. The liquid crystal is confined between two plates. The top (bottom) plate has strong (weak) anchoring. The horizontal state can be switched to the vertical state by an electric field. Then, if the field is abruptly switched off, one might expect the system to relax back to the horizontal state. The relaxation commences at the boundaries, where the molecules start to rotate in the same direction at the top and bottom surfaces. If one does not consider the effect of the backflow (equivalent to using a Ginzburg–Landau equation to describe the dynamics), then this is indeed the case, as shown by the simulation results in Fig. 4. (The simulation parameters are summarized in [18]. Backflow is switched off by setting the velocity to zero in Eq. (3).)

If, however, backflow is included, a horizontal flow is created starting from the top plate and gradually reaching the bottom surface. This horizontal flow causes the molecules to rotate in the opposite direction at the bottom surface. As a result the vertical state transforms to a bend state, as shown in Fig. 5. There is an energy argument which suggests that the bend state is unstable and quickly relaxes to a twist state [17] if the Frank elastic constant K_{22} is sufficiently small compared to K_{11} and K_{33}.

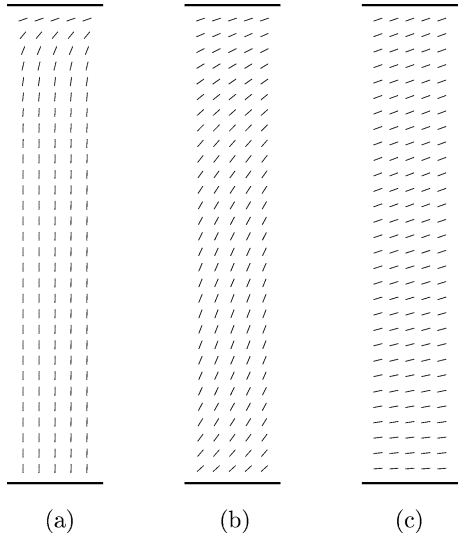

Fig. 4. Snapshots of the director configuration of the surface switching device after the electric field is switched off, but backflow effects are not incorporated in the model. The (a) vertical state relaxes through (b) an intermediate state to (c) the horizontal state. The snapshots correspond to 0, 7 and 15 ms. At the top surface the molecules are strongly pinned at a 20° pretilt to the horizontal axis. Pinning at the bottom surface is weak with a 0° pretilt.

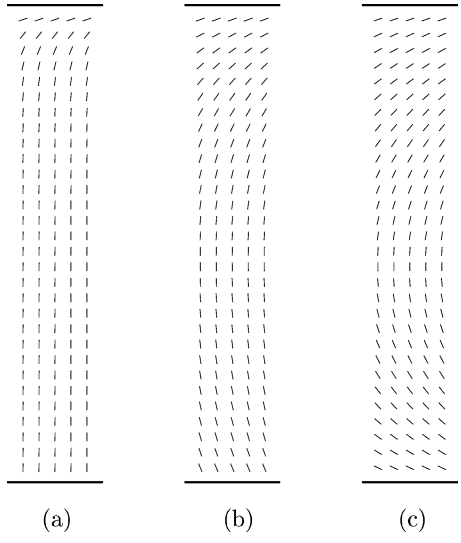

Fig. 5. Snapshots of the director configuration of the surface switching device after the electric field is switched off, and backflow effects are incorporated in the model. The (a) vertical state relaxes through (b) an intermediate state to (c) the bend state. The snapshots correspond to 0, 1 and 6 ms.

Hence in a bistable device, if the field is switched off gradually, the effect of back-flow is weak, and the liquid crystal settles in the horizontal state. If the field is switched off abruptly, then it settles in the twist state. When a field is reapplied both zero field configurations switch back to the vertical state.

6. Conclusion

In conclusion, we have derived and implemented a lattice Boltzmann algorithm for liquid crystal hydrodynamics. This opens the way to investigate a wide range of physical phenomena which result from the coupling between the director field and the flow, many of which have been examined only indirectly or with severe approximations in the past. Two examples have been presented showing the relevance of flow to switching in liquid crystal devices.

Acknowledgements

We thank E. Acosta for helpful conversations. Financial support from the EPSRC is acknowledged.

References

[1] P.G. de Gennes, J. Prost, The Physics of Liquid Crystals, 2nd edn., Clarendon Press, Oxford, 1993.
[2] R.G. Larson, Constitutive Equations for Polymer Melts and Solutions, Butterworths series in Chem. E, Butterworth, 1988.
[3] P.D. Olmsted, C.-Y. David Lu, Phys. Rev. E 60 (1999) 4397.
[4] S. Chen, G.D. Doolen, Annual Rev. Fluid Mech. 30 (1998) 329.
[5] M.R. Swift, E. Orlandini, W.R. Osborn, J.M. Yeomans, Phys. Rev. E 54 (1996) 5041.
[6] J.M. Yeomans, Ann. Rev. Comp. Phys. VII (1999) 61.
[7] A. Lamura, G. Gonnella, J.M. Yeomans, Europhys. Lett. 45 (1999) 314;
O. Theissen, G. Gompper, European Phys. J. B 11 (1999) 91.
[8] A.N. Beris, B.J. Edwards, Thermodynamics of Flowing Systems, Oxford University Press, Oxford, 1994.
[9] M. Doi, S. Edwards, The Theory of Polymer Dynamics, Clarendon Press, Oxford, 1989.
[10] L.D. Landau, E.M. Lifshitz, Electrodynamics of Continuous, Pergamon Press, New York, 1960.
[11] C. Denniston, E. Orlandini, J.M. Yeomans, Phys. Rev. E 63 (2001) 056702.
[12] F. Brochard, E. Guyon, P. Pieranski, Phys. Rev. Lett. 28 (1972) 1681.
[13] The director field is an order parameter giving the average local direction of the molecules. It lies along the largest eigenvector of **Q**.
[14] The parameters used correspond to: a starting voltage 5.6214 V, 0 V during relaxation, $\epsilon_{\parallel} = 19$, $\epsilon_{\perp} = 5.2$, $\gamma_1 = 0.15$ Pa s; Meisowicz viscosities $\eta_1 = 0.17$ Pa s, $\eta_2 = 0.04$ Pa s, $\eta_3 = 0.04$ Pa s, $\eta_{12} = 0$; elastic constants $K_{11} = 11.1$ pN, $K_{22} = 6.7$ pN, $K_{33} = 17.1$ pN; pretilt at surface 2°, cell thickness 3 μm.
[15] The Ericksen–Leslie equations (J.L. Ericksen, Phys. Fluids 9 (1966) 1205; F.M. Leslie, Arch. Ration. Mech. Analysis 28 (1968) 265.) are hydrodynamic equations of motion for nematics written in terms of the director field. The Beris–Edwards equations considered in this paper reduce to them for a uniaxial order parameter of constant magnitude.
[16] J. Kelly, S. Jamal, M. Cui, J. Appl. Phys. 86 (1999) 4091.
[17] I. Dozov, M. Nobili, G. Durand, Appl. Phys. Lett. 70 (1997) 1179;
J.G. McIntosh, F.M. Leslie, J. Eng. Math. 37 (2000) 129.
[18] Parameters used correspond to: sample width 1.7 μm; $\Gamma = 3.33$ Pa^{-1} s^{-1}, $L_1 = 8.75$ pN, $L_2 = 6.36$ pN and $L_3 = 13.60$ pN (or equivalently $K_{11} = 4.83$ pN, $K_{22} = 3.24$ pN, $K_{33} = 8.23$ pN); Miesowicz viscosities 0.02 Pa s to 0.15 Pa s.